LL

EUROPEAN ORGANIZATION FOR NUCLEAR RESEARCH
European Laboratory for Particle Physics

CERN - ST DIVISION

CERN-ST-95-06

CERN ST/95-06 (IE)

LHC Note 360

Superconducting or resistive cables for the supply of the LHC magnets

M. Teng

Abstract

This note discusses the possible use of superconducting links to supply the LHC magnets and compares such links with conventional cables. Technical feasibility and the implications of both types of solution are discussed. Owing to space constraints imposed by the existing underground structures a conventional cable solution renders the construction of new alcoves necessary at points 1 and 5.
The feasibility study was ordered from two specialized companies and has resulted in two design proposals for superconducting links. Finally, a cost comparison shows the difference between the price of superconducting links and conventional cables.
A recommendation to proceed further with the industrial development of a prototype concludes this report.

Geneva
Switzerland
July 1995

ST/Div. Rep.

Contents

1 INTRODUCTION

The LHC will be built in the existing LEP tunnel. This puts constraints on the dimensions of the equipment for the new machine as space inside the tunnel is limited. The construction of new experimental areas and the enlargement of existing caverns cannot be avoided. However, to reduce costs, civil engineering underground will be limited as much as possible and the machine systems' design will take this into account.

Most of the magnets of the LHC will be high-current, low-voltage, superconducting, and cooled to 1.9 K by superfluid He. The cryogenic cooling needed requires extensions of the existing LEP cryogenic cooling systems. Since cryogenic installations will be available for the machine cooling it is natural to consider whether the connections from the power converters to the magnets could be made superconducting as well.

This note presents a comparison between conventional and superconducting cables for the connections between the magnets and the power converters. It also indicates at which access points this choice is relevant.

Concerning the application of superconducting cables, there are some unknowns. This note will try to identify them.

For the resistive solution, the major problem is the available space. Additional civil engineering may be necessary in some situations.

The total implications, costs, and benefits of choosing a certain solution should be compared, not simply the costs of the cables themselves. Therefore the questions which will be addressed by this note are:

1) Is the use of superconducting links between the power converters and the magnets technically feasible and
2) if so, then where could they be used?
3) Is there an economic and/or technical advantage compared with the conventional alternative?

The answer to the last question requires a complete cost overview of the conventional cable solution.

2 BACKGROUND

The electrical powering requirements of the LHC magnets and the LEP magnets are completely different. Contrary to the LEP magnets, the LHC magnets have high-current and low-voltage needs. The LHC will therefore require a different powering system from that of LEP. This concerns the power converters themselves, but also the cabling; cable cross-sections will be large and lengths limited. Insulation voltages will be rather low, a few kV at the most.

From a supply point of view, the initial LHC machine design foresaw almost equal powering needs for each of the eight access points. Each point catered for the complete cryogenic and electrical supply, from the intersection point to mid-arc, to both sides. At points containing a low beta insertion the powering needs were slightly higher.

At an early stage it was recognized that the installation of the LHC power converters on the surface was not feasible. The connections between the power converters and the magnets would be as long as 450 m: 250 m underground, 100 m vertically, and 100 m on the surface. Very high losses would result, leading to unacceptable running costs.

To keep distances short and reduce losses the power converters had to go underground, close to the machine connection interfaces (the feedboxes). At the odd points this meant

additional civil engineering, as space is insufficient near the dispersion suppressor feedboxes, located 250 m from the intersection point. Underground civil engineering being expensive and risky should preferably be avoided, provided alternatives are available.

The decision to dismantle LEP before building the LHC alleviated the problem of space at the even points. The RF galleries will be used to house the power converters. Since these galleries end close to the arc and dispersion suppressor feedbox, resistive cable lengths from the power converters to the magnets can be short. Superconducting links at the even points are thus no longer interesting.

The 8-point supply implied much underground civil engineering at the odd points. At points 3 and 7 the new structures served only to house the cryogenic and power supply equipment.

Then, the so-called four-point feed was introduced aiming, amongst other advantages, at lessening the required civil engineering. It is based on supplying the main bending and lattice quadrupole magnets (circuits with large currents) from the even points, across mid-arc.

The powering needs of points 3 and 7 have been drastically reduced compared with the original powering scheme. Initially comparable with points 1 and 5, they now require less than one ninth of the current of these points. This can be seen by comparing the currents shown in Figs. 1 and 2.

Figure 1 shows the distribution of currents amongst the different circuits at point 3. Each column corresponds to circuits with the rated current indicated below it. The height is equal to the rated current multiplied by the number of circuits, giving the total current for the indicated rating.

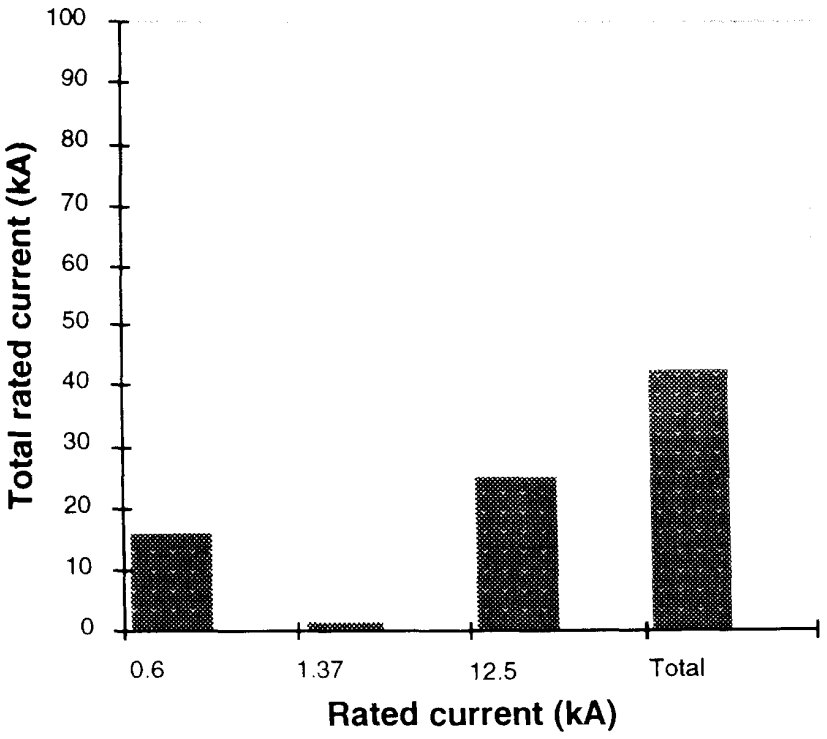

Fig. 1: Circuit currents at point 3.

The circuits with rated currents less than or equal to 50 A have been left out. They are dedicated to corrector magnets and connected locally. The 12.5 kA discharge circuits represent the largest portion of the total current carrying capacity. These discharge circuits

are the counterparts of the main bending supplies at the even points, and consist of a switch, closed in its normal position with a dump resistor in parallel. The total column is the sum of the other columns.

The total rating of the local power converters is about 18 kA. Including the two 12.5 kA discharge circuits gives the total cable rating of 43 kA.

Because of the current reduction at points 3 and 7, superconducting links will have a limited application at these points, if at all.

The first experiments will be built at points 1 and 5. They require low beta insertions and strong focusing. Strong focusing is achieved with high-gradient quadrupole magnets in the dispersion suppressor which are powered locally. They are connected through the feedbox for the dispersion suppressor. Contrary to points 3 and 7 this represents a number of high-current circuits that have to be fed locally. There are no galleries available as there are at the even points.

As will be shown in Chapter 3 dissipating cables cannot bridge the distance to the central cavern, because of the losses. Therefore new alcoves are needed to permit the power converters to be located nearby.

Underground civil engineering would be reduced at points 1 and 5 if superconducting cables could be used. The power converters could be located further away, without the dissipation problems mentioned earlier.

Figure 2 shows the circuit current data for point 5. The first column for each circuit rating represents the case of a central, superconducting solution. It is based on the series connections of identical circuits left and right of the intersection point (see Table 1).

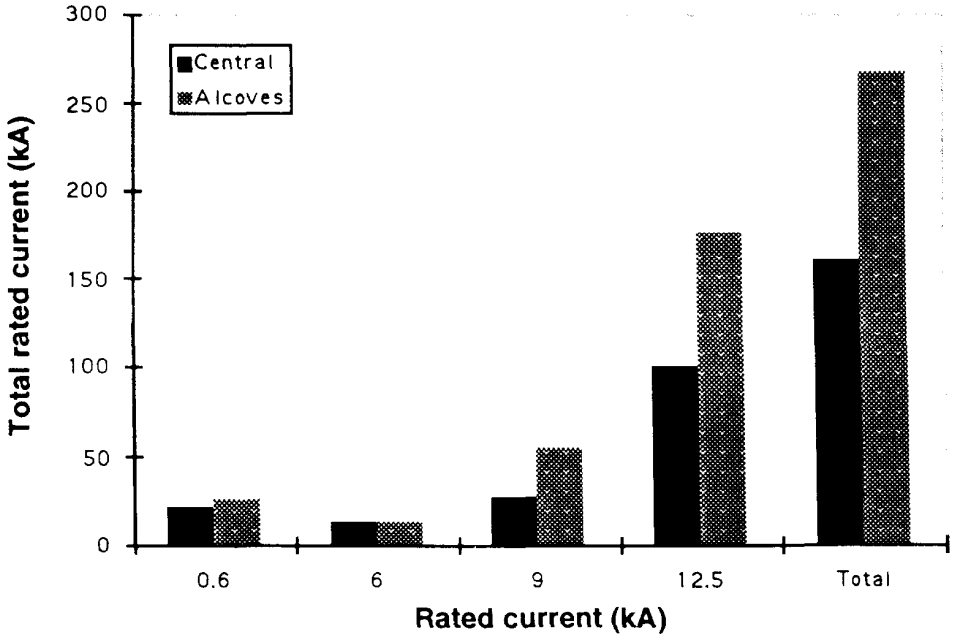

Fig 2: Circuit currents at point 5.

The second column represents the resistive alcove solution, without series connections.

These columns can also be interpreted as the necessary current rating for the busbars and the superconducting links for either series connections, or single connections.

The 'Total' column is directly related to the rating of the power converters with the two discharge circuits added. It is much higher than at point 3: 267 kA for a resistive solution, and 161 kA for a central solution. These numbers include the two discharge circuits.

Data for these graphs have been extracted from the powering lists, to be published in the forthcoming 'White Book' update.

In view of the construction needs and the current ratings, points 1 and 5 are the most interesting candidates for superconducting links. This report will focus on these points.

Table 1 lists the circuits to be supplied at these points. In some cases, superconducting links allow series connections between left and right circuits. The number of these circuits is also given.

Table 1: Magnet circuits at points 1 and 5

			Feedbox				
Function	Circuit	I (kA)	Dispersion Suppressor left	Low beta left	Low beta right	Dispersion Suppressor right	Series conn. possible
Outer triplet	Q4,5,6	12.5	6			6	6
Skew quadrupoles	Qs4,6,8,10	0.6	8			8	8
Trim quadrupoles	Qt7,8,9,10	0.6	8			8	
MB discharge	MB	12.5	1			1	
Separator	D1	9		1	1		1
Separator	D2	9		2	2		2
Low beta	Q1–3	6		1	1		
Low beta trim	Qt1,3	0.6		2	2		
Low beta	Dipole corrector	0.6		4	4		

3 CABLING ALTERNATIVES AND THEIR IMPLICATIONS

3.1 Description of structures and systems at points 1 and 5

Powering

This paragraph only deals with access points 1 and 5 which are the only likely candidates for superconducting links.

Figure 3 shows the machine connection points, the so-called tunnel feedboxes (TFB), and their distances from the intersection point (X). At 60 m a feedbox connects to the low beta insertion, and at 250 m another one connects to the dispersion suppressor. The feedboxes contain the current feedthroughs which transports the current from ambient temperature to low temperature.

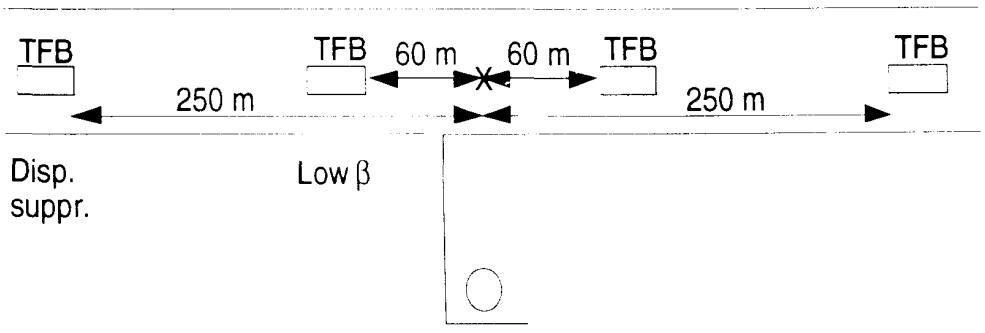

Fig. 3: Location of machine connection points at a low beta point.

The problem of space has already been mentioned. The main problem is the supply of the dispersion suppressor. For the low beta insertion the problem is similar, but on a smaller scale.

Installing water-cooled cables to bridge the distance from the central cavern to the dispersion suppressor feedbox could be considered. The following example illustrates the consequences for such a case.

The largest currents are about 12.5 kA. This is too much for one 750 or 950 mm^2 cable, so this current will be shared amongst several cables. Let us suppose that 2.5 kA is being passed through a 750 mm^2 Cu water-cooled cable, over 285 m. Dissipation P is given by: $P = i^2\rho l/A = 40.4$ kW. To keep the water temperature increase down to 20 K a flow of

$$\frac{40.4\ \text{kW}}{4.2\ \text{kJ/kgK} \times 20\ \text{K}} = 0.48\,\text{kg/s}$$

is needed.

The diameter of the water tube inside the cable is 12 mm. The flow of 0.5 l/s through this tube of 285 m length requires a pressure drop of 65 bar. The normal working regime of the pumps is around 5 bar. Alternatively, several water circuits per cable are needed. The current to be transported at the odd points with low beta is of the order of 160 kA.

This explains why a dissipating cable over a long distance is not feasible, even when the cable is water cooled. The operating losses become tremendous and a large water cooling installation is needed.

Lengths of about 250 m are too long for only one cooling circuit, so each cable has to be cooled by multiple water circuits. The cable package with all the water feeding tubes is bulky. To reduce cable length the solution is to put the power converters close to the feedbox 250 m inside the new alcoves.

Thus the cabling alternatives in this situation are:

1) conventional cabling, together with the construction of new alcoves,

2) superconducting links.

With superconducting links the power converters can all be located in the central cavern. The feedboxes, which contain the feedthroughs from ambient temperature to 4.5 K, can also be located in the central cavern. They may even be combined, thus reducing costs. The possibility therefore exists to connect circuits left and right in series, which is not possible with the alcove option. Figure 4 shows an example of an odd point with the power converters located in the central cavern. Figure 5 shows the corresponding power supply diagram. The current sources represent the power converters.

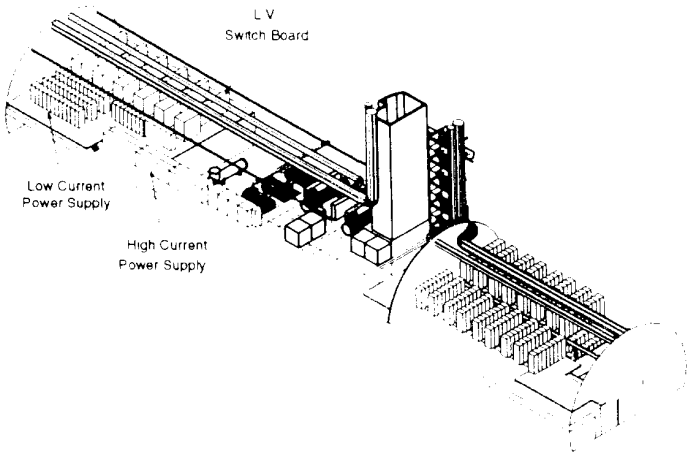

Fig. 4: Power supply location in a central cavern.

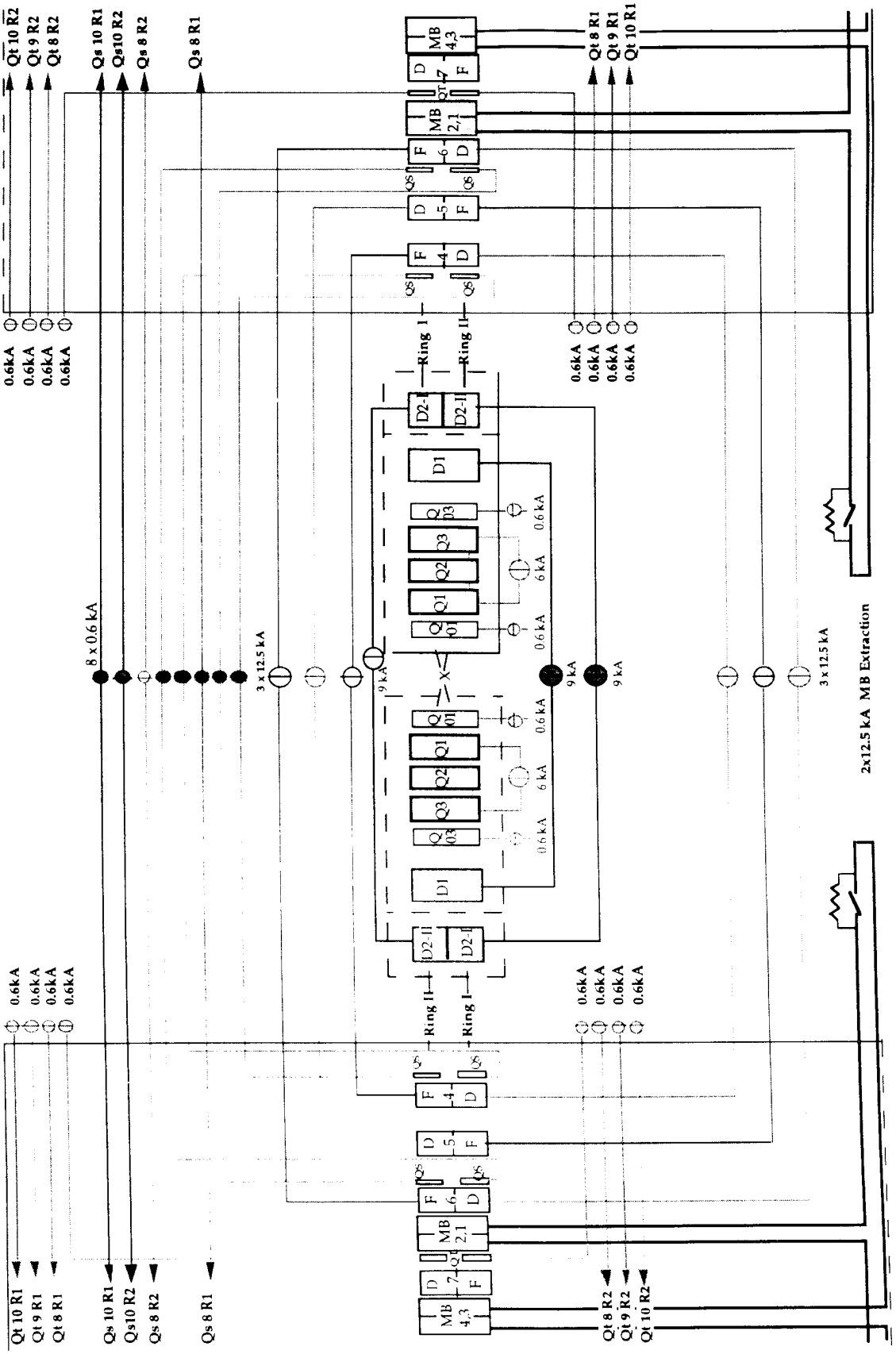

Fig. 5: Powering diagram for points 1 and 5.

Cryogenic installations

LEP phase 2 is already equipped with four cryogenic refrigerators, with an output power of 12 kW at 4.5 K each. The equipment is located at the even points. The operation principle for liquefaction is the so-called Claude cycle. It consists of the Brayton cycle, combined with a Joule–Thomson valve. It is a continuous flow process with rotating machines, as is usual for large power cryogenic plants. A more detailed description is given in Appendix A.

For the LHC an expansion is planned in order to increase the power of each of the plants to 18 kW and to supply the odd points from the adjacent even points. Figure 6 shows a diagram of the principle of the LHC cooling plants. Helium is cooled in several stages from 300 K to 1.8 K. In the process it passes through the warm compressors, the upper cold box (UCB), and the lower cold box (LCB). The cryoplant interconnect box distributes to the left and right sides. Helium at 4.5 K, 2.5 bar is delivered to the TFB, where 1.8 K is produced to cool the magnets. The primary cooling of the magnets will be by 1.8 K pressurized He (1 bar). This is produced by pumping He to 16.3 mbar, resulting in two-phase He boiling at 1.8 K. The cold compressors which do the pumping are located inside the compressor cold box (CCB). The tube in which the He boils at 1.8 K is in thermal contact with the magnet cold mass, which is kept at 1 bar.

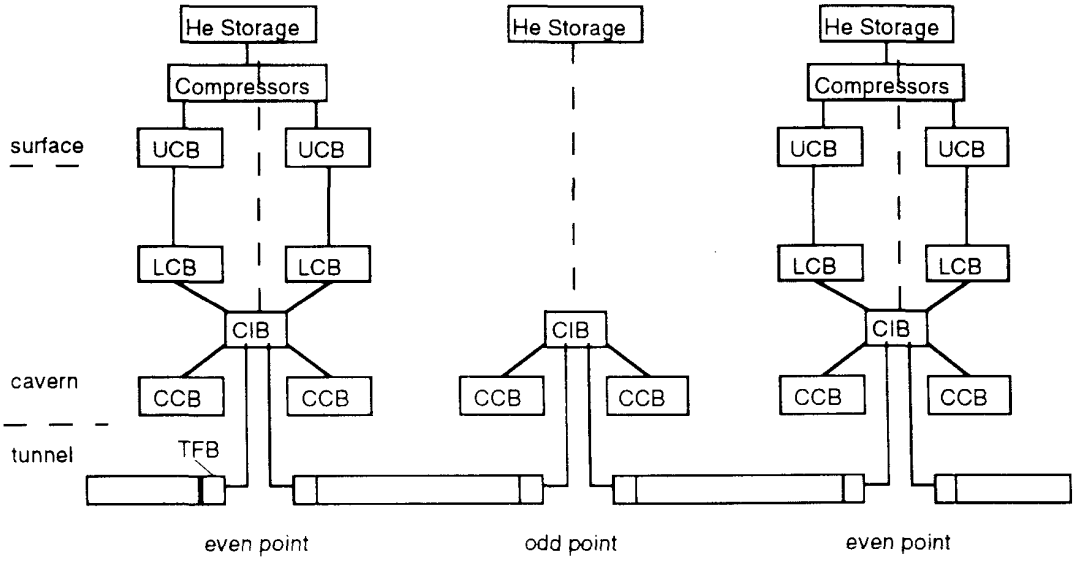

Fig. 6: Cryogenic installations for the LHC.

3.2 Resistive cables

The alcove solution: description of the cabling

As it has been shown, resistive cables require alcoves 250 m from the intersection point. The total current of the circuits in the alcove, rated 600 A or more, is about 85 kA. For the cables this means 170 kA to be transported, to and fro. Increasing the current density reduces the necessary space at the expense of a higher dissipation.

An optimum must be found, given the available space, between the amount of cables installed and the running costs. Using copper cables with a current density of 4 A/mm^2, which approaches the limit, the dissipation per metre of the total package is almost 12 kW.

To get an idea of the cable cross-section, the required number of 240 mm^2 Cu cables, with a diameter of 35 mm, is 180. This corresponds to 12 full cable ladders, each 60 cm wide.

The heat dissipation of the cables, for the situation shown in Fig. 7 with normal copper cables is 235 kW (see Table 2). The data are for the alcove only. This Table is not extremely precise: the number of cables mentioned was obtained by dividing the total Cu cross-section by the cable cross-section. Nevertheless, it gives a good idea of the order of magnitude of the heat to be removed. The number of cables would be greater in reality, as some cables will be used only fractionally.

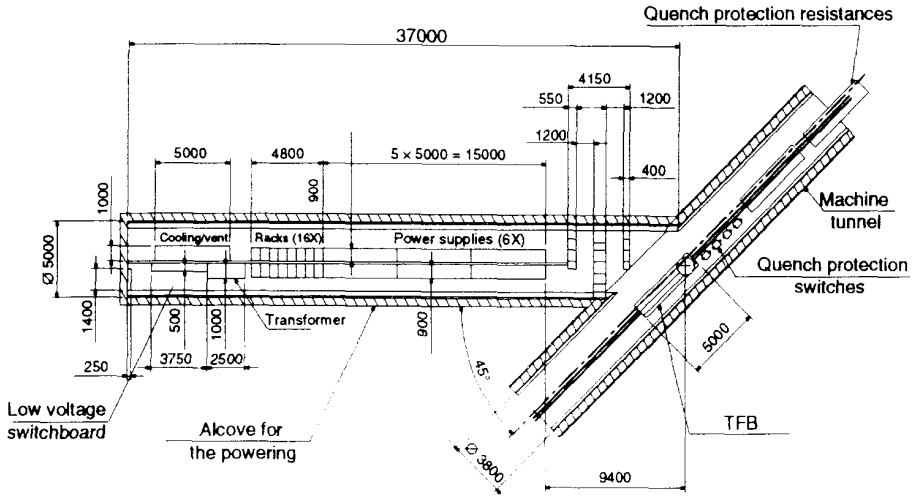

Fig. 7: Alcove for resistive cables only.

Cabling of the discharge circuit is not taken into account because for the resistive solution the discharge switches are very close to the feedbox, inside the machine tunnel.

Table 2: Air-cooled cables

Circuits	Current (A)	Cable x-sect. (mm^2)	No. of Circuits	Distance (m)	Dissipation (kW)	Current (kA)
Outer	12500	12500	2	14.4	49	50
Triplet:	12500	12500	2	19.4	66	50
Q4,5,6	12500	12500	2	24.4	83	50
Qs/Qt	600	2400	8	27.5	18	9.6
	600	2400	8	29.5	19	9.6
	TOTAL	42300 *)			235	169

*) No. of 240 mm^2 cables: 178

The dissipation of 235 kW is far too much to be extracted by means of air; 25 kW would be reasonably acceptable. A reduction to about 30 kW would already require eight times as much copper, impossible to install in the available space.

Therefore, despite the reduction in length due to the alcoves, the heat will still have to be dissipated into water, using water-cooled cables.

Water-cooled cables are well known at CERN. For long lengths, the function of water cooling is not to boost the current-carrying capacity, but simply to extract the heat. In this case, an important difference with regular power cables is the extra need for space; the cables are larger and require a water circuit.

The operating current of a water-cooled cable depends on the maximum water temperature increase, normally 20 K, and thus, on the length of the cable and the water flow. The length and the flow are directly related to the pressure drop.

Using water-cooled cables with a maximum current density of 3.33 A/mm^2 results in a dissipation of 180 kW in the circuits fed from the alcove, as listed in Table 3a. This table is more precise than Table 2; the number of cables required is calculated per circuit. It shows a solution using water-cooled cables for all circuits.

The number of 3.33 A/mm^2 is an optimum value between Cu costs and running costs. The current density of 1.5 A/mm^2 for the 600 A circuits is explained by the following: the smallest available water-cooled cables have a cross-section of 400 mm^2. Another 74 kW is dissipated in the connection to the low beta insertion. Table 3b contains data on the cables of Table 3a and their costs. Total connection costs (end pieces plus cables) amount to 550 kCHF.

Table 3a: Cabling with water-cooled cables only: dissipation

Function	Current (A)	J (A/mm^2)	Cable x-sect. (mm^2)	Circuits	Distance (m)	Dissipation (kW)	Current (kA)
Alcove							
Outer	12500	3.33	15000	2	14.4	41	50
Triplet:	12500	3.33	15000	2	19.4	55	50
Q4,5,6	12500	3.33	15000	2	24.4	69	50
Qs/Qt	600	1.50	6400	8	27.5	7	9.6
	600	1.50	6400	8	29.5	7	9.6
TOTAL			57800			179	169
Low beta Insertion							
D1,D2	9000	2.40	22500	3	25	55	54
Q1–3	6000	2.67	4500	1	25	14	12
Qt, Dcorr.	600	1.50	4800	6	25	5	7
TOTAL			31800			74	73
Half point total:						252	242

Table 3b: Cabling with water-cooled cables only: installation costs

	Parallel cables per connection		Total number of cables		End pieces		End pieces	Cost per metre	Cost of cables	Connection cost
	750 mm^2	400 mm^2	750 mm^2	400 mm^2	750 mm^2	400 mm^2	(CHF)	(CHF)	(CHF)	(kCHF)
Alcove										
	5		20		40		52000	165	9504	62
	5		20		40		52000	165	12804	65
	5		20		40		52000	165	16104	68
		1		16		32	36800	119	52360	89
		1		16		32	36800	119	56168	93
Low beta										
	5		30		60		78000	165	24750	103
	3		6		12		15600	165	8250	24
		1		12		24	27600	165	17850	45
TOTAL CONNECTION COST										549

Optimization of the alcove solution

Table 4 shows the cost overview after optimization. The 600 A circuits are now cabled using air-cooled power cables of 240 mm^2 cross-section. Part of the heat, 12 kW, is now dissipated in air. The savings are about 200 kCHF, with total cabling costs down to 353 kCHF per half point. Dissipation in the cavern is almost equal at 177 kW, compared to 179 kW previously. This includes the 12 kW dissipated in air.

Table 4: Optimization, cabling with water-cooled cables, and air-cooled cables: installation costs

	Parallel cables per connection		Total number of cables		End pieces		End pieces	Cost per metre	Cost of cables	Connection cost
	750 mm^2	240 mm^2	750 mm^2	240 mm^2	750 mm^2	240 mm^2	(CHF)	(CHF)	(CHF)	(kCHF)
Alcove										
	5		20		40		52000	165	9504	62
	5		20		40		52000	165	12804	65
	5		20		40		52000	165	16104	68
		2		32		0	0	26	11440	11
		2		32		0	0	26	12272	12
Low beta										
	5		30		60		78000	165	24750	103
	3		6		12		15600	165	8250	24
		2		24		0	0	26	7800	8
TOTAL CONNECTION COST										353

The origin of most of the savings can be explained as follows. The end pieces for water-cooled cables are expensive, more than 1000 CHF each, including fitting. Two are needed for each cable. A 10 kA connection requires two times four cables of 750 mm^2, and 16 end pieces.

Civil Engineering

The required additional alcoves, close to the connection feedbox of the machine, will house the powering equipment for the dispersion suppressor. Each alcove will have a diameter of 5 m; enough for two rows of 0.9 m racks with a standard height of 2.2 m in the middle. The length of the alcove will be 35 m. This space is sufficient for electricity distribution equipment, cooling and ventilation installations, and the power converters.

The machine tunnel will be enlarged locally to facilitate the connection of the 5 m diameter alcove. The costs of civil engineering are outlined in Table 5.

Table 5: Costs of civil engineering

Item	Description	Price (kCHF)
1	Alcove tunnel 5 m dia. × 35 m length	950
2	Demolition and temporary support of existing machine tunnel	300
3	Enlarged machine tunnel section 5 m dia. × 10 m length	300
4	False floor steelworks	50
	TOTAL	1600

The prices quoted for the first three items include 15% for installation of the works site and 5% engineers' fees.

Figure 7 shows a drawing of the alcove, including the positioning of the power equipment. The alcove will not be perpendicular to the machine tunnel. This facilitates entering the power and cooling and ventilation equipment. The drawing does not show the machine tunnel enlargement over a section of 10 m.

The low beta insertion will be fed from the bypass tunnels at point 1 and from the UJ56 enlargement, point 5 right (see Fig. 8). The left low beta at point 5 requires a new passage not indicated in the figure to avoid long cable lengths. This passage runs from the central cavern (US) to the machine tunnel, with a bend in it to act as a shield to avoid radiation from the machine. The power converters for this low beta will be in the central cavern. The cost for this passage is 160 kCHF.

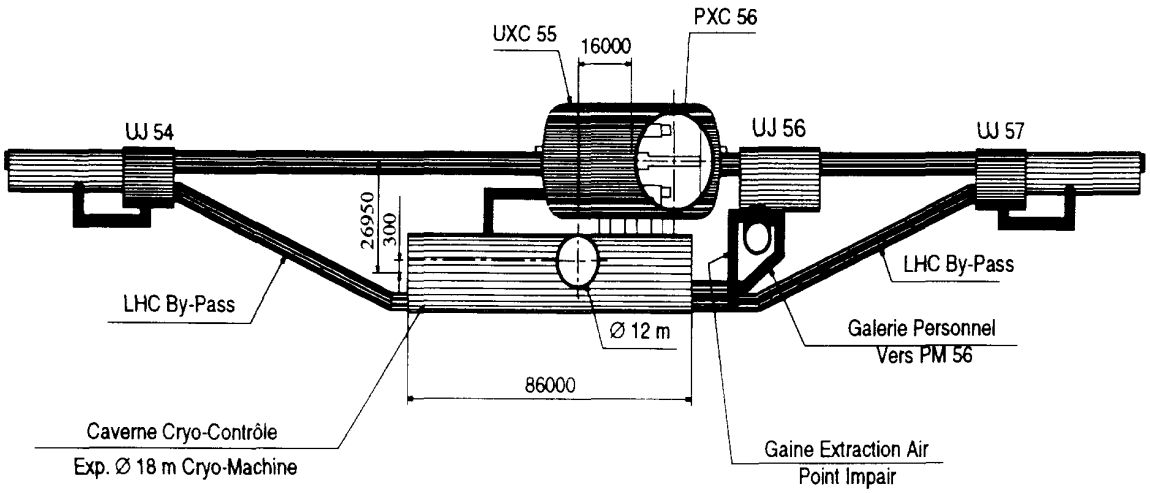

Fig. 8: LHC point 5 as foreseen.

Cable routing from the alcove to the machine

The cables have to cross the machine in the main tunnel. This involves either running the cables close to the ceiling or under the false floor.

The preferred option is to route them close to the ceiling as this results in the shortest lengths. Routing the cables under the false floor would add about 1.5 m to the lengths. Eventually, the convection-cooled cables could be under the false floor. The low-current density in these would allow the longer length without major consequences.

A full-size feedbox is required inside the tunnel to provide the transition from the cold He to the ambient temperature. The possibility of putting similar circuits left and right of the intersection point in series is lost and therefore the full number of power converters will be necessary.

Cooling and ventilation

The dissipation of cables and powering equipment in the alcoves is 600 kW. Like the cables, the power converters will be water cooled. The water-cooling equipment can be installed at the rear of the alcove. As an indication, costs for a cooling plant of 500 kW cooling capacity are about 300 kCHF. The additional cost for 600 kW will be less than 20%, since these do not scale linearly.

Discussion

The use of resistive cables implies a massive use of water-cooled cables to extract the dissipated heat. It has been shown that, using normal power cables, too much heat is dissipated in the air inside the alcove.

The advantage of the alcove solution is that no further development is needed for the connection from the power converters to the tunnel feedbox. It is all known technology.

A number of disadvantages are apparent. There are two more alcoves per point, with the uncertainties connected with underground civil engineering.

From the operational point of view, the important disadvantage is the loss of access to the power converters: during machine operation no access will be possible. If a breakdown occurs it will take time before access can be granted. A stop due to an equipment fault, located in an alcove, will be of considerable duration.

The feedbox will necessarily be a full-size one, placed inside the machine tunnel where space is limited. As such it may have to be built around the machine beam pipes, making it very hard, if not impossible, to access the inside part of it after installation. Shifting the tunnel enlargement so that its centre does not coincide with that of the machine tunnel could result in an additional gain in space for the feedbox. It is not certain that this will be sufficient. The feedbox does not form part of the study.

3.3 Superconducting links

Industrial expertise

The design of the superconducting cables and their environment requires a knowledge of both electrical and cryogenic engineering, and feedback from a number of areas. A part of this knowledge has to come from outside CERN, particularly where manufacturing capabilities are concerned. It was therefore decided that industry should be asked to make a proposal and a cost estimate for the superconducting links. The comparison and evaluation should be made by CERN.

A technical note defining the situation was written. It described the configuration of the LHC at that time, including the corresponding magnet powering needs. It laid down the boundary conditions of an electrical and cryogenic nature, and those imposed by the geometry. It posed a number of questions giving direction to the study. This note was then used as a basis for discussion with two industrial partners already involved in superconducting magnet developments for CERN.

Using the results of the discussions, a specification for a design study was made [1]. This study was then used to obtain the necessary knowledge from industry. The specification defined all the known boundary conditions and stipulated, in detail, what should be covered by the study.

Manufacturing and installing cryogenic equipment is completely different from manufacturing superconducting wires and cables. Not many companies had knowledge and experience in both areas so partnerships were established to complement knowledge. The companies contacted were:

- ABB
- Alsthom
- Ansaldo
- Siemens KWU

• Siemens MBG
• Oxford Instruments

Alsthom co-operated with Kabelmetal Electro.
Ansaldo teamed up with Linde.
Oxford Instruments was the only firm with all the required knowledge in-house.

Specification

At the time of the specification, the design of the LHC was changing rapidly. In order not to waste time trying to follow the developments, it was decided to base the specification on the machine as it was documented in the 'White Book' [2].

Since, in this design, the underground space at the odd points was by far not sufficient to house the power converters, it was assumed that the superconducting cables for the study would have a vertical section of about 150 m. In this way, the power converters could be housed on the surface.

The study was not directed towards implementation at any access point in particular. It was recognized that the machine design was still evolving. Therefore, an imaginary standard access point was conceived, including the difficulties identified in the preceding technical note. These were, amongst others, a vertical section of 150 m, a total circuit current of 107 kA per half point, cryogenic stabilization, and survival of a main dipole circuit discharge in the absence of cooling.

The usefulness of the results was assured by imposing the inclusion of complete derivations of the formulae used in the final report. This would allow CERN to adapt the results to a changing machine design later on.

Progress, follow up

After a call for tenders, two firms were selected to perform the design study: Kabelmetal–Alsthom and Oxford Instruments. Midway through the study (November 1994) oral presentations were made to inform CERN of progress, and to give an opportunity to exchange ideas.

At the midway presentations, it was decided to adapt some aspects of the study to the actual design of the machine which, in the meantime, had become a four-point feed design. This design eliminated the need for vertical sections. Consequently, the requirement of a 150 m vertical section for the study was dropped. This was essential, since the tolerable height appeared to be around 90 m at the most, due to the hydrostatic pressure loss.

The currents of the different circuits were not adapted as they were already close to the actual machine design. Table 6 shows the difference between the study and the current machine configuration. The 10 kA currents have risen to 12.5 kA, but a number of circuits have had their rated currents reduced from 1.6 kA to 600 A. The overall figure remains about the same as for the alcoves. If the MB discharge circuit is included, the current for superconducting links rises to 97.1 kA. This is about 10 kA above the current in the study which will have to be accounted for, either by flexibility in the design, or by a connection scheme that reduces the effective current. Provided this is possible, the data from the study are still valid for comparison with the current machine.

Table 6: Current from the power converters

Study			Alcove pt. 5		
Current (kA)	Occurrence	Circuit	Current (kA)	Occurrence	Circuit
12	1	Main	12.5	–	Discharge MB
10	5	Outer triplet Q	12.5	6	Outer triplet Q
1.6	12	Qs/Qt	0.6	16	Qs/Qt
0.7	2	6/10 pole			
0.6	2	Qt			
0.5	8	6/8 lattice			
Total one-way current 87.7 kA			Total one-way current 84.6 kA		

General implications

If superconducting cables are applied the powering can be simplified. The power converters can all be located at a distance from the machine feed point. The logical place would be the central US cavern, which will house services to the experiment, electricity distribution, cryogenic installations, and cooling equipment. Some circuits of identical functions, left and right of the intersection point, can be powered in series. This reduces the quantity of power converters needed. The dump resistors and quench protection switches can be located at a distance, instead of inside the machine tunnel.

Resistive connections

Superconducting links still require resistive connections from the power converters to the feedbox. Provided dissipation can be kept sufficiently low, it may not be necessary to use water-cooled cables in all of the circuits. More space will be available and more copper cross-section can be installed than for conventional cables.

Tables 7a and 7b list the costs of the warm cables to connect the power converters to the superconducting links. The numbers in these Tables are for the whole point; for comparison with a half point they must be divided by two. For these cables the actual currents are assumed, as with the resistive cable solution.

Table 7a: Water-cooled cables central cavern, complete point

	Parallel cables per connection		Total number of cables		End pieces		End pieces	Cost per metre	Cost of cables	Connection cost
	750 mm^2	400 mm^2	750 mm^2	400 mm^2	750 mm^2	400 mm^2	(CHF)	(CHF)	(CHF)	(kCHF)
Alcove										
	3		24		48		62400	165	6600	69
	3		24		48		62400	165	9240	72
	3		24		48		62400	165	13200	76
		1		52		104	119600	119	92820	212
Low beta										
	3		18		36		46800	165	9900	57
	2		8		16		20800	165	6600	27
		1		24		48	55200	121	7260	62
TOTAL CONNECTION COST										575

Table 7b: Water-cooled and air-cooled cables central cavern, complete point

	Parallel cables per connection		Total number of cables		End pieces		End pieces	Cost per metre	Cost of cables	Connection cost
	750 mm^2	240 mm^2	750 mm^2	240 mm^2	750 mm^2	240 mm^2	(CHF)	(CHF)	(CHF)	(kCHF)
Alcove										
	3		24		48		62400	165	6600	69
	4		32		64		83200	165	9240	92
	4		32		64		83200	165	13200	96
		2		104		0	0	26	20280	20
Low beta										
	3		18		36		46800	165	9900	57
	2		8		16		20800	165	6600	27
		2		48		0	0	26	9360	9
TOTAL CONNECTION COST										370

Table 7b gives the optimized costs with standard power cables conducting the smaller currents. The drawback is a dissipation of 35 kW into the air for a complete point; this is 17.5 kW for a half point. The cost of resistive cables is now 370 kCHF for the whole point. Note that this is a similar optimization to the one applied for the resistive cable solution.

Tunnel Feedbox

The tunnel feedbox[1] can be made simpler compared with the resistive cable solution. It becomes a connection box reduced to its cryogenic function, without an He bath for the feedthroughs. Electrically it will house the connections between the magnet busbars and the superconducting cables. The actual feedboxes with the feedthroughs are moved to the central cavern.

The feedboxes for both sides of the intersection point can be combined, provided a mechanism is available to control the flows individually. This allows series connections of certain circuits, left and right of the intersection, reducing the number of feedthroughs.

4 DETAILS OF THE PROPOSAL BY KABELMETAL ELECTRO–ALSTHOM

The Kabelmetal Electro–Alsthom design is based on separate, dedicated conductors per magnet circuit. These conductors are wrapped together, forming one big multicore, multipurpose cable. Furthermore, the superconducting cryogenic links to feed the arc are separate from those feeding the insertion. The assembly of cables and cryogenic envelope is flexible, and can be prefabricated in 75 m pieces.

Cryogenic link design proposals

The two studies have resulted in two different design proposals. The following sections discuss both of them in detail.

[1] Please note that the historical name *cryo feedbox*, used in the drawings, is referred to as *feedbox* in this report. Since it is not purely cryogenic, but rather a symbiosis between an electrical and a cryogenic connection, the preferred name is feedbox. If it sits in the tunnel it becomes *tunnel feedbox*.

Cryostability

The conductor diameter and the Cu:SC ratio, R_S = Cu/SC are determined by the condition of cryogenic stability, also known as the Stekly criterion, using the formulae elaborated in Appendix B: *Verification of formulae used by KE–Alsthom.* The value for the heat exchange from the cables to the He is estimated to be 4000 W/m^2, as with the He bath cooling with 50% of the conductor area in contact with the He. The company expects a better value from forced-flow supercritical He cooling.

The field on the conductor is not expected to exceed 1 T. This gives a T_C of 8.8 K. The RRR of the copper is 100 at 4.5 K. Table 8 is based on this data and is taken from their report.

Table 8: Cu/SC Ratios and diameters of cryostable conductors

	I_{op} (kA)	Cu/SC	Diameter (mm)
ARC			
Main magnet	12	36	13.9
Disp. Sup. Q	10	33.8	12.3
Skew/Tuning Q's	1.6	18.4	3.7
6/10 poles	0.7	13.9	2.2
Trims	0.6	13.2	2
6/8 poles	0.5	12.5	1.8
Insertion Feedbox			
Int. Separator D1	8	31.4	10.6
Low beta Q1–Q3	5	26.9	7.84
Int. Separator D2	5	26.9	7.84
Trims	0.6	13.2	1.97

Adiabatic temperature rise

One of the boundary conditions is to sustain a total quench discharge in the absence of cooling, without damage. This situation can occur when the cryogenic plant fails. Assuming adiabatic conditions results in finding the upper limit of the temperature rise. To calculate the heat increase Alsthom applied a method similar to the MIITS integrals (Appendix A). However, using this method to determine the necessary amount of Cu results in conductors too large for the available space in the cryogenic envelope, even with a rise of 400 K.

During their presentation, Alsthom discussed this matter at CERN. Because of their enormous discharge time constant of 120 s, only the main discharge circuits run into limitations as far as temperature rise is concerned. However, during this time, the remaining He, the surrounding conductors, and the cryogenic containment, can all take some of the generated heat, resulting in a lower conductor temperature. Therefore the adiabatic assumption does not reflect reality, but gives a pessimistic view.

Alsthom strongly advised a higher adiabatic temperature rise in order not to make the big cables larger than necessary. Using a rough estimate, and taking the surroundings into account, the maximum temperature is shown to be limited to 350 K.

Wires, conductors, and insulation

Table 9 contains the dimensions proposed by Alsthom based on the constraints and calculations. The conductors consist of superconducting strands and an additional amount of Cu strands, in order to reach the correct Rs. The required insulation level is 2 kV. According to Alsthom, this is not very hard to achieve. They intend to use two layers of Mylar or Kevlar foil, with a thickness of 0.25 mm for two layers.

Table 9: Proposed conductors

Nominal current	12 kA	10 kA	1.6 kA	0.7 kA	0.6 kA	0.5 kA	2 × 4 kA	5 kA
Maximum field (T)	1	1	1	1	1	1	1	1
Cu/SC ratio, overall	35.0	35.0	19.2	12.5	12.5	12.5	29.3	29.3
No. of SC strands	38	24	4	3	3	1	10	10
Strand dia. (mm)	1.2	1.2	1.2	1.25	1.14	1.76	1.3	1.3
Cu/SC strand	7.0	7.0	7.0	12.5	12.5	12.5	7.0	7.0
Filament dia. (μm)	52	52	52	49	45	69	56	56
No. of Filaments	66	66	66	48	48	48	66	66
Twist pitch (mm)	20	20	20	25	25	35	25	25
SC area (mm^2)	5.36	3.38	0.56	0.27	0.23	0.18	3.32	1.66
Cu area (mm^2)	187.5	118.3	10.8	3.4	2.88	2.25	97.3	48.6
Critical current (4.5 K) I_c (A)	32160	20280	3360	1620	1380	1080	19920	9960
Op. current I_{op} (A)	12000	10000	1600	700	600	500	2 × 4000	5000
I_{op}/I_c	0.37	0.49	0.48	0.43	0.44	0.46	0.40	0.50

Contraction

The conductors will be helically wound around a centre element. The pitch of the helix shall be such that the radial shrinkage of the centre element compensates for the longitudinal shrinkage of the wires. In this set-up, the cryogenic envelope could be fixed without causing strain to the conductors at cool-down. The calculation for the pitch is elaborated in Appendix B. The Alsthom–Kabelmetal report mentions the radial movement and distance change between wires. The numbers are confirmed, using a slightly different approach from the formula they mentioned (Appendix B). In case of a sudden pressure increase, the shrinking element passes He in the axial direction.

Cryogenic envelope

The cryogenic containment proposed, consists of four corrugated tubes of increasing diameter, fixed inside each other in a recursive manner, as shown in Fig. 9. The production process limits the dimensions for the outermost tube to 198 mm inner diameter, and 220 mm outer diameter. All tubes inside have subsequently smaller dimensions and, as a consequence, the innermost tube can have a maximal diameter of 75 mm. The cryogenic lines going to the low beta insertions will be of smaller dimensions, but are otherwise the same. Starting from the centre, the spaces inside and between the tubes contain respectively:

- 4.5 K He + superconducting cable,
- superinsulation and vacuum,
- 70 K screening He,
- superinsulation and vacuum.

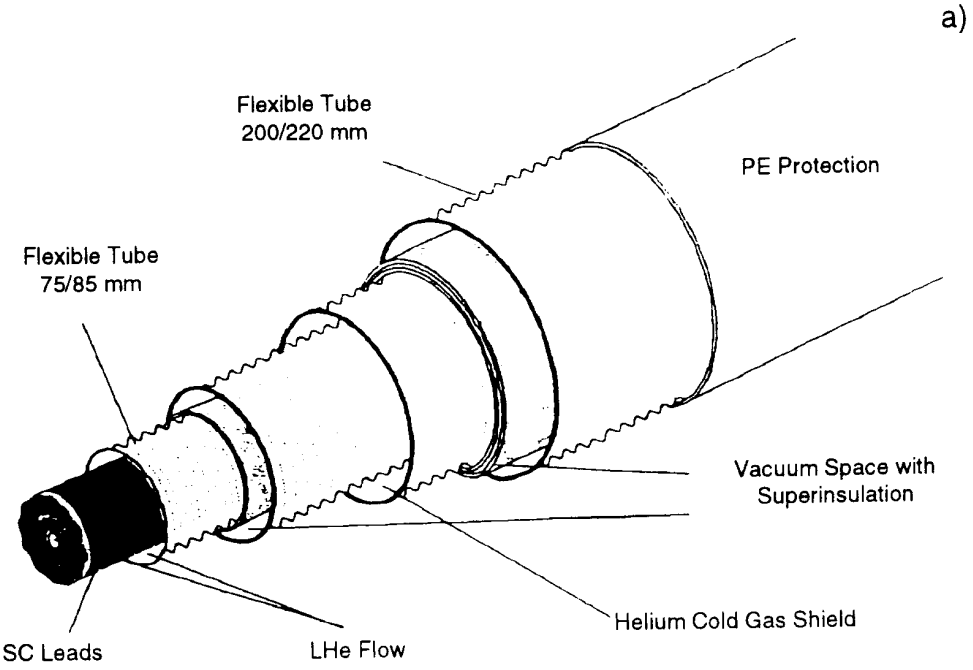

Fig. 9: Flexible superconducting cryogenic link.

The ARC Link consists of 4 corrugated tubes with the following diameters:
Inner tube: 75/85 mm–100/110 mm
130/147 mm–198/220 mm
There is a cooling screen with cold He gas for low heat inleak to the innermost LHe tube. It has an outer diameter of 130 mm and an inner diameter of 110 mm. The inner tube contains the SC Cable ± with the superconducting leads.
The LHe flows inside the 75 mm inner tube and within the gaps of the SC Cable. About 5 layers of superinsulation (40 µm Al and spacer material) reduce the heat inleak to 0.2 W/m at a shielding temperature of 50–75K or 0.05 W/m at a shielding temperature of 5–20K.
The He cold gas shielding in the space between tube 100/110 and tube 130/147 is separated by a vacuum space from the inner LHe flow and from the surroundings.
For a good insulation of the shield gas there is a high vacuum space with about 30 layers of superinsulation (12 µm Al coated polyester foil and spacer material) around it to limit the heat inleak to 2.5 W/m. To avoid direct contacts between the tubes some special spacers will fix the tube position in the centre. The spacers must be able to take the weight and the bending forces of the cable.

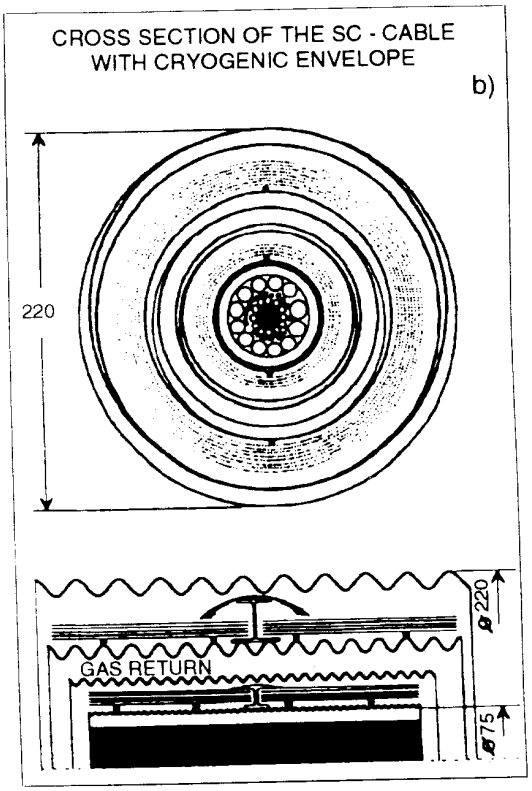

Cooling conditions, stability issues

Given a flow of He of 8 g/s, needed for the feedthroughs, the Reynolds number can be found and subsequently the heat transfer coefficient, h. These are respectively 5900 and 174 W/m^{2}K. For the main dipole conductor, Alsthom assumed the value of 960 W/m^2 K. The difference lies in a different method of calculating the Reynolds, as elaborated in Appendix A. Discussions on this topic have taken place with KE. The preliminary conclusion is that the exact value can only be determined by a prototype measurement.

In Fig. 10 below, the heat transfer coefficient is shown as a function of the temperature. Because of a change of the He properties, at 5.3 K there is a steep increase of h. The figure is drawn for a mass flow of 8 and 16 g/s. This shows that an increase of the flow results in a better heat transfer. Furthermore, a slight increase in temperature also results in a better heat transfer, provided the temperature stays below 5.3 K. This figure was computed using HEPAK data as input.

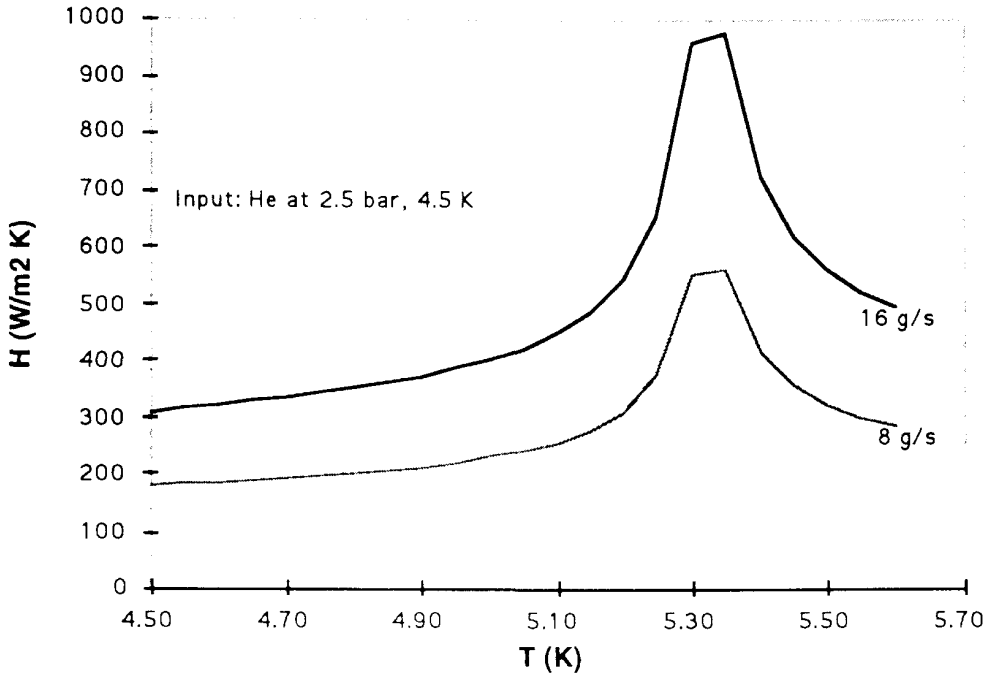

Fig. 10: Heat transfer coefficient.

Discussion

The construction chosen by KE–Alsthom is very attractive in terms of manufacturing and installation. The cables can be produced and pre-tested at the production site in lengths of 75 m. This greatly facilitates installation in the tunnel. The design is elegant in that the cables and the inner and outer tubes do not move with respect to each other at cool-down. They can be fixed together at multiple points along the link. Similar constructions have been used before. Most recently, as a full scale prototype for the Japanese LHD [3].

The design of the superconducting cable and its cooling are rather critical. The adiabatic temperature rise calculation shows an increase of more than 450 K. This is not serious since it is recognized that heat exchange will occur during discharge thus limiting the final temperature. The influence of the insulation is not accounted for, and this could give an additional temperature difference of 1 to 2 K. The corrugated tubes are costly: 2550 CHF per metre.

During discussions, the subject of cross-talk was raised. KE–A had located the go and return conductors diametrically opposite each other to reduce the forces. This results in a maximal coupling between adjacent circuits. With a ramp rate of 10 A/s the induced voltage is 1.58 mV. A reduction of eight times is possible by having adjacent conductors for go and return current for each circuit. The error ratio now becomes 10^{-5}. Appendix A contains elaborate calculations on coupling between circuits for the solution proposed by KE–A.

The error caused by this effect is a step function throughout the ramp. Since the power converters will be controlling the current, an integrating action of the control system can easily cancel this. This means that a PI or PID controller will adjust the driving voltage to obtain a zero-steady state error.

Prototypes

Two prototypes are proposed, one for the arc and one for the insertion link, each with a length of 20 m. Because of production limitations, a superconducting cable of 20 m is too short for the foreseen fabrication method. The alternatives are: a 20 m handmade cable prototype, or 100 m of cable production, cut to 20 m, to test the production facilities as well. The prototype costs are outlined in Table 10. Prices are based on an exchange rate of 1 DEM = 0.85 CHF. The prototypes do not include connection boxes. A manufacturing time is not given.

Table 10: Proposed prototypes and their costs

	Cable length (m)	Price (kCHF)
ARC	20	220
	100	305
Insertion	20	65
	100	90

KE–Alsthom propose a number of tests:

- material tests (RRR, Ic) to be performed on the wires and cables,
- connection losses and time to make connections,
- tests on the performance of the contraction principle,
- stability tests under different operating conditions,
- critical current determination,
- temperature rise upon discharge without cooling of the main bending magnets circuit,
- mechanical tests of insulation materials,
- cool-down measurements,
- heat losses,
- pressure drops,
- flow capacity.

At least one additional test will be necessary to prove the cooling assumptions in order to verify the heat exchange coefficient. For example, this can be done with a full-scale model, heating one conductor and measuring its temperature under normal flow conditions. Taking a bare conductor and in another case an insulated one, allows the effect of the insulation to be determined as well.

In the concluding remarks, KE–Alsthom mention that they are absolutely confident of the technical feasibility of their design.

5 DETAILS OF THE PROPOSAL BY OXFORD INSTRUMENTS LTD

The proposal of Oxford Instruments is based on a single-wire type; wires are twisted in pairs and connected in parallel to obtain sufficient current-carrying capacity. This approach results in a considerable flexibility of choice for the currents to be conducted, and with little to no extra costs the design may be adapted to a different configuration of currents. Mass fabrication of the wires can be applied. The wires are insulated individually and have to be connected individually. The cryostat is of the rigid type, as for the LHC magnets. It has sufficient space to house the cables feeding the arc, as well as those feeding the insertion. Because of the rigid outer cryostat, the cable and the cold part of the cryostat must be free to move at cool-down.

Cryostability

For the conductor design a cooling of 3100 W/m^2 by convection is assumed by OI. See Appendix A for calculations with respect to this number. The conductors are individually electrically insulated. The temperature drop across the insulation is taken into account throughout the calculations. It is given by:

$$\Delta T_{ins} = \frac{Q \ln (2t/d)}{2\pi k} \quad .$$

The subsequent transfer of heat to the He can be expressed by:

$$\frac{Q}{l} = h\pi (d + 2t) \Delta T_{surface} \cdot$$

The dissipated heat per metre during a transition to ohmic state is:

$$\frac{P}{l} = I^2 \frac{\rho}{s} .$$

where

ΔT_{ins}: temperature drop across insulation (K)
Q: heat flow (W)
P: dissipated power (W)
I: current (A)
t: insulation thickness (m)
d: conductor diameter (m)
h: heat transfer coefficient (W/m^{2}K)
k: thermal conductivity (W/mK)
r: copper resistivity (Ωm).

These flows of heat must be equal and result in a conductor temperature below the critical temperature, Tc, Tc ≈ 10 K, to ensure cryogenic stability. The RRR for the copper is 100. These conditions lead to Table 11 which was taken from the OI report. A wire diameter of 2 mm is proposed. For smaller wire diameters the amount of insulation gets relatively large and for larger diameters the relative surface of the wire gets smaller, which means that cooling decreases.

Table 11: Conductor parameters for various diameters

Wire diameter (mm)	Q (W/m)	ΔT_S (K)	I (A)	J (A/mm^2)
1	0.310	0.28	40	50.5
2	0.563	0.33	107	34.0
3	0.815	0.35	193	27.3
4	1.07	0.37	294	23.4

Adiabatic temperature rise

The adiabatic temperature rise is limited to 100 K. The formula used is similar to the MIITS calculations, and the outcome of the integral according to OI is equal to 780 MIITS/cm^4. In the Table in Ref. [4] it is 791 MIITS/cm^4. These calculations only apply to the main dipole circuit; all other circuits have much lower discharge time constants. Consequently, for these the cryogenic stability criterion is more severe than the adiabatic temperature rise.

Wire, conductor, cable

The 2 mm wires are insulated for 2 kV, either by wrapping about four layers of Kapton® tape total thickness around 0.25 mm, or by extrusion of Stilan. Extrusion would result in a thickness between 0.15 and 0.20 mm. Since the insulation also causes a heat resistance, from the cooling point of view it is best to keep it as thin as possible.

The insulated wires are then twisted in pairs. To reduce cross-coupling and self fields, wires of a pair are always connected to the same circuit, conducting currents in opposite directions. The maximum field in a wire pair is 36 mT. The twisted pairs are bundled into cables of 85 pairs. One such cable has an overall capacity of more than 18000 A. To transport the currents to the arc, 10 such cables are needed. For the insertion currents an additional three are necessary, making a total of 13.

Contraction

Because of the rigid design of the cryogenic envelope, the complete inner part will move at cool-down. Shrinkage is 0.33%, or 0.825 m on a 250 m length. Just in front of the connection to the machine, the cable enters a contraction box where it is wound in a helical shape. When the cable contracts this helix works like a spring. Inside the helix is a core of polymer foam, for mechanical support and for volume reduction.

Cryogenic envelope

The cryogenic envelope is a transfer line made of 15 m sections. These sections are joined by junction boxes. The cable package is supported by rolling spacers with brass rollers. From the cold 4.5 K mass, the design subsequently shows vacuum space, the 50 K screen, vacuum, and the vacuum case (Fig. 11). The cold vessels are allowed to move. This movement is compensated by bellows which connect them to the junction boxes. The design also envisages the connection of magnets in series left and right from the intersection point, allowing separate control of the He flows. Elaborate calculations were made on the heat loads, giving a necessary minimal He flow of 8.35 g/s, per half feedbox.

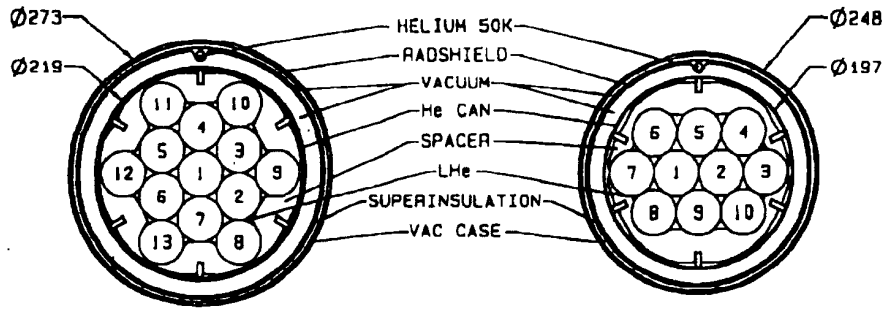

Fig. 11: Superconducting link layout.

Operation

This section is dedicated to operation under normal and under fault conditions.

Under normal conditions, He (4.5 K, 2.5 bar) is lead into the transfer line at a flow rate of at least 8.35 g/s. Capturing heat, 21.8 W, over the transport length of 300 m, it arrives at 4.9 K at the feedbox in the central cavern. Here it passes through a Joule–Thomson valve and expands into 1.2 bar, temperature 4.4 K. The liquid fraction after expansion is 84% mass. Flow is controlled with a warm valve, after the feedthroughs, which vaporize and heat the He to room temperature. Screening He at 50 K is taken from the connection box in the tunnel as for the He at 4.5 K. It screens the transfer line and the feedbox. It is then heated to room temperature and passes a warm valve, keeping the flow at 15 g/s.

The fault conditions discussed are: interruption of 50 K and 4.5 K supply, and loss of vacuum. A quench of the link, after having lost cold supply, is shown to be non-destructive. The feedbox buffer of liquid helium is sufficient to sustain more than 100 minutes of operation, in case of an interruption. In the event of a loss of vacuum the He has to be vented to keep the pressure down. Bursting discs are incorporated in the design to allow the venting.

Manufacturing

The estimated manufacturing completion date is two years after reception of the order, plus three months for installation. This time is based on applying superconducting links to eight points. It depends largely on the production of the superconducting cable as other production steps can be done in parallel. From this, two points would take about one year, including installation. This is based on the assumption that because of the parallel processing of wires, cables, and cryogenic equipment, to do one quarter of the job takes half the time. The full completion dates before delivery have to be counted from several sub-contractors.

Discussion

The design of OI is very flexible and easily adaptable to different current configurations. The twisted pairs lead to low forces and little fields. The report is very detailed and covers all the necessary items, including the temperature drop on the insulation. The design is rather conservative, giving it good prospects for technical success.

The cooling calculation of the wires is based on the cooling of a single wire. It remains to be verified whether this approach is valid for a total package of numerous wires. It is easy to increase the coolant flow, should this be necessary. Insulating the wires by extrusion can reduce the thickness of the insulation layer, increasing the stability. A single wire type makes mass production possible. The design incorporates a margin which may be needed to cope with the changes of the currents.

The on-site assembly of the cryogenic vessels is a disadvantage. This, in addition to the design margins, increases the price.

Prototype

A prototype is proposed consisting of two 15 m transfer line sections, with one junction box. The wires are all connected in series and fed with a 97 A current; the total current thus becomes 214 kA. Tests are proposed to check the heat load, the insulation, and cryogenic and adiabatic stability. The delivery time is one year for manufacturing and testing, and the cost is about 500 kCHF.

6 COMPARISON

Table 12 contains a comparison of the various options, applicable to one half point. These data are graphically represented in Fig. 12. Cable data on the resistive, or warm solution, are optimized for equipment positioning. Power cables are taken as part of the installation. Superconducting links are part of the equipment. Except for the use of normal copper cables for the lower currents instead of water-cooled cables, it is not possible to economize more by shortening the cable length or similar variations. This optimization has been taken into account.

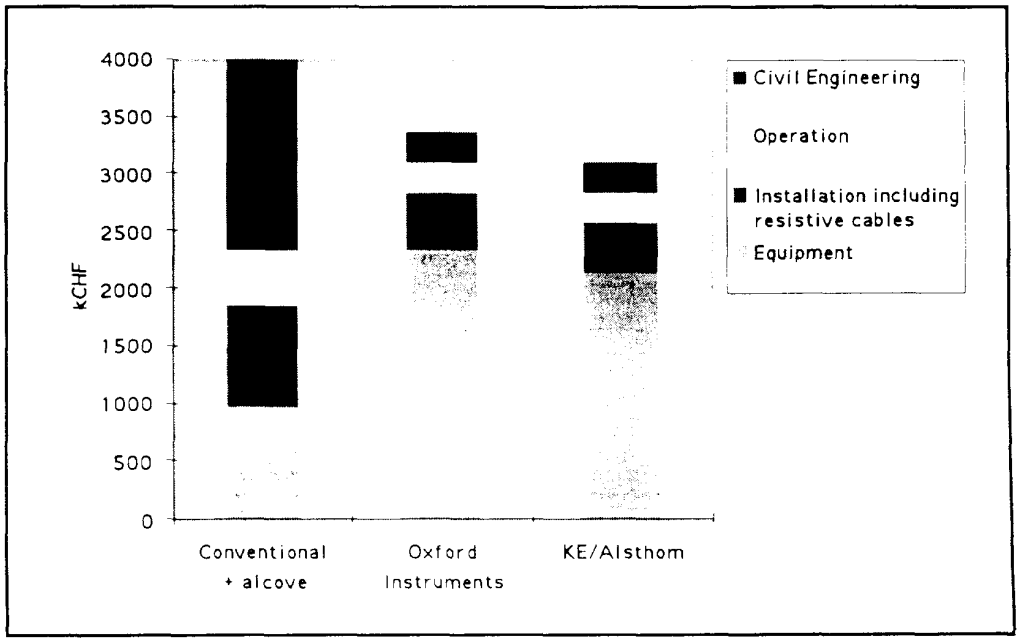

Fig. 12: Comparison of cabling alternatives: costs for one half point.

The central, superconducting solutions, with all power converters in the US cavern, can be further optimized. It will be relatively easy to reposition the equipment, compared to Fig. 4, reducing cable lengths of the largest currents between the power converters and the connection to the superconducting cables. Already a similar optimization as for the conventional cables has been taken into account for the numbers in Table 7b. It consists of using normal power cables for the smaller currents.

The added complexity of having a tunnel feedbox in the warm solution is estimated at 200 kCHF. The costs of the proposed solutions of OI and KE–Alsthom depend very much on the prototype results. The feedthrough prices are based on a fixed price per Ampere, with the existing vapour-cooled feedthroughs at SM18 used as a reference.

Cable costs include supports, end pieces, and installation. Losses are capitalized over a period of seven years of operation, 3500 hours yearly. Heat loads of the transfer lines and the feedthroughs are less than the feedthroughs only, for the resistive solution. They are therefore not taken into account. Dissipation of the resistive solution is 312 kW, and for the superconducting solution 139 kW.

Maintenance applies only to the cooling and ventilation equipment and is therefore very limited. Maintenance of superconducting links should be very low, as for the cryogenic transfer lines, but is not known exactly.

The cost of the construction of an alcove is estimated at 1400 kCHF. The space taken in the central US for the whole point is estimated to be 520 kCHF. Per half point this becomes 260 kCHF. This is a pro rata estimate, based on the total costs of the cavern, and does not take into account the fact that the tunnelling equipment has to go down in any case.

Care must be taken when interpreting these figures. The prices for the superconducting links do not include development. The complication and duplication of the feedbox are not completely included in the resistive solution.

If the changes of the machine design since the White book are taken into account, the differences between the conventional and the superconducting solutions become larger. The OI design already incorporates a sufficient margin to handle the larger currents without changes. The KE–Alsthom design will have to be adapted, but will not become more expensive than the OI proposal. The larger currents increase the operating losses and require more cables, in particular in the low beta connections. Overall, the superconducting solutions will be more interesting as current increases.

7 PROTOTYPES

Two main reasons for building prototypes are:

- construction and manufacturing verification and
- measurements to verify the behaviour and performance under various conditions.

Prototypes will at least test the cryogenic stability and heat transfer in the chosen geometry. Further tests will involve:

- temperature rise in case of a discharge,
- loss measurements,
- contact resistances,
- functioning of the safety system in case of a malfunction such as the loss of cooling power or loss of vacuum.
- Autonomy of the feedbox in case of a loss of cooling power.

8 CONCLUSION, RECOMMENDATION

8.1 Conclusion

It goes without saying that the possible economic gain of using superconducting current links has been reduced by a factor of four, compared with the machine design at the end of 1992. The reduction from eight to two points of possible application is the cause for this lower gain.

It has been shown that a conventional cable solution is only feasible if additional caverns are built at points 1 and 5. These will cost 1.4 MCHF each. Owing to the location, cooling the cables by water is the only way of extracting the heat, resulting in overheads of

400 kCHF for the cables and the additional water treatment and circulation equipment. Furthermore, the access to power supplies will be impossible without switching off the beam and a controlled access procedure.

On paper the superconducting solutions appear cheaper than the conventional solution. The gain when applying one of these is about 2.8 MCHF. This must be offset against the cost of development. It will amount to between 500 kCHF and 1 MCHF. This solution has no access problem.

The use of SC links avoids the problem of space that dominates the resistive cables solution.

The proposal by KE involves more risk, but could lead to a cheaper solution in the end. The solution offered by OI is more conservative, more expensive, and more laborious. Owing to the conservative design, it is easier to adapt the cooling and the current configuration.

It is difficult to judge which of the superconducting designs is better. Both have their strengths and weaknesses.

With regard to costs of the superconducting links, both companies involved have made estimates with reservations. The actual cost also depends on the results of tests made on one or more prototypes.

Neither company could provide proof of technical feasibility on paper, in particular as far as cooling conditions and stability are concerned. Clearly, this can only be verified with a suitable model.

The cryogenic needs of the lines are small, compared to the feedthroughs. The reduction of feedthrough cooling needs makes up for cooling of the superconducting links.

8.2 Recommendation

Apart from the practical implications, there appears to be a financial gain in the use of superconducting links. There is no proof of technical feasibility on paper, and a prototype is needed to verify the cooling conditions. The heat exchange and thus the respect of the Stekly criterion was not proven. It is therefore proposed to have both companies make a crude prototype, to first prove their cooling assumptions. Sufficient references exist to ensure their capability of producing the superconducting wires the way they propose.

The heat exchange in the given set-up should be confirmed, by measuring, for example, the temperature of a wire, conducting current in a similar geometry as the companies' proposals.

The decision to continue development with further prototypes is therefore based on the outcome of this test of the heat exchange.

If the result of this test is positive, the proposal is to have one or more prototypes, according to the manufacturers' descriptions. These will then serve to check the manufacturing techniques and to assess performance under various conditions.

The possibility of constructing the two alcoves per point will, however, be reserved until a final decision has been taken. This decision will be taken after studying the prototypes.

The information contained in this report was based on the parameters known at the time of writing it.

Acknowledgements

I would like to thank J. Pedersen for his stimulating support and his efforts when checking the draft versions. I would also like to thank the many others who have helped me to make this document what it has become.

REFERENCES

[1] M. Teng, Technical specification for a design study of superconducting links for LHC. ST–IE–GD DO–14838/ST, April 1994.

[2] Large Hadron Collider – The Accelerator Project CERN/AC/93–03 'White book'.

[3] T. Mito, T. Uede, M. Ikeda et al., Development and tests of a flexible superconducting bus-line for the large helical device, IEEE Trans. Magn. **30** (1994) p. 2090–2093.

[4] M.S. McAshan, MIITS Integrals for Cu and for Nb 46.5wt%Ti, SSC–N–468.

[5] Z.J.J. Stekly and J.L. Zar, Stable superconducting coils, IEEE Trans. Nucl. Sci. **23** (1965) p. 367–372.

Table 12: Comparison of resistive and superconducting cables.Two superconducting solutions offered by Oxford Instruments and Kabelmetal Electro–Alsthom. Per half point (point 1.5).

	Resistive		Superconducting			
		kCHF	Oxford Instruments	kCHF	Kabelmetal Electro–Alsthom	kCHF
Equipment	Additional power converters	500	Cryo, superconductor, misc.	2100	Cryo, superconductor, misc., no conn. box	1400
	Tunnel Feedboxes added complexity	200			Conn. Boxes	500
	Feedthroughs	280	Feedthroughs	230	Feedthroughs	230
Installation	Extra: 2 tunnel feedboxes		System	100	System	50
CV(≈ 1MW heat)		500		250		250
Cables		360		185		185
Operation (7 years, 3500 hrs/yr)						
Losses	Electrical (kW)		Electrical (kW)		Electrical (kW)	
Cables	303		139		139	
Cooling and vent	9		4.5		4.5	
Total	312		144		144	
Associated costs		380		176		176
			Thermal load for 300 m*)		Thermal load for 350 m**)	
			23 kW	28	22.44 kW	27
Heat load FT						
(= at 4.5 K Wth)	65 kW	80	53 kW	65	53 kW	65
Associated costs	240.6 Wth		196.8 Wth		196.8 Wth	
Civil Engineering	Alcove	1600	Extension US	260	Extension US	260
Additional construction						
	Cost (rounded)	3900		3400		3100

*) 87.2 mW/m (4.5 K)
2.5 W/m (50 k)
**) 50 mW/m (4.5 K)
2.5 W/m (50–70 K)

APPENDIX A

Explanation of the terms used

Cryogenic stability: the Stekly criterium

The Stekly criterium for cryogenic stability [5] demands that in the course of a local transition to the Ohmic state (Fig. A.1) the dissipated heat becomes less than the heat transfer to the surroundings, at a temperature below the critical temperature of the superconductor. This assures that under normal cooling conditions, the temperature of the conductor never rises above this equilibrium temperature.

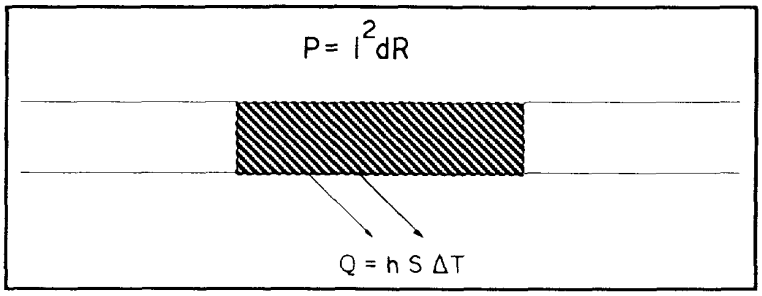

Fig. A.1 Local transition to the Ohmic state.

Stability depends on dissipation, on cooling, and on the critical temperature in the given circumstances (B,I,J). Dissipation can be reduced by using more matrix material, usually Cu, but Al is also used.

Cooling depends on the active surface, S, the temperature difference between surface and coolant, ΔT, and the heat exchange coefficient, h. This coefficient depends very much on the type of cooling and the flow type of the medium.

Calculation of the heat transfer coefficient

For heat exchange by convection, to calculate h one must first find a value for Nusselt's number, Nu, which is given by:

$$Nu = \frac{hd}{k},$$

where

d: hydraulic diameter
k: heat conductivity.

The expressions for forced flow are in general:

$$Nu = aF\, R_e^{m}\, Pr^{n},$$

where Reynolds, R_e, characterizes the flow type, laminar or turbulent, Prandtl, Pr, characterizes heat mobility, and a, F, m, n are coefficients depending on the geometry and flow type. The Reynolds number depends on the geometry and on the flow speed.

The Reynolds is determined by the following:

$$R_e = \frac{\rho v D}{\eta} = \frac{\dot{m} D}{S\eta},$$

where

S: flow surface
η: viscosity
D: hydraulic diameter; D = (4S/P), where P = wetted perimeter
$\dot{m}$: mass flow.

Given the mass flow, it can be seen that the Reynolds depends purely on the wetted perimeter, P. It is a measure of interaction of the gas with the walls surrounding it. If $R_e > 4000$ the flow is turbulent, if $R_e < 2000$, it is laminar.

Prandtl is a function of physical parameters of the medium and does not depend on the geometry. Prandtl can be obtained once the temperature and pressure of the He are known.

Prandtl indicates the heat mobility by convection or conduction, or rather the inverse of the heat mobility. A lower Prandtl means that heat moves more easily, a higher Prandtl means that heat is more trapped in one spot.

$$Pr = \frac{\eta c}{k}.$$

For the case of a cylinder, forced flow, the coefficients to calculate Nusselt are as follows:

$$Nu = 0.023\, R_e^{\,0.8}\, Pr^{0.37}.$$

This is also known as the Colburn formula.

For natural convection the Reynolds number is no longer important. In this case the Grashof number, indicating the upward movement of particles, due to heating, against inertia and viscosity, becomes a determining factor:

$$Gr = \frac{\alpha g \Delta T D^3}{\eta^2}, \qquad \alpha\rho = \frac{d\rho}{dT}.$$

And the Nusselt number is a function of Gr and Pr: $Nu = a\,(Gr \cdot Pr)^n$. The characteristic distance D depends on the case. It is the distance that the particles carrying the heat travel. For a cylinder it is the diameter. For two parallel horizontal plates it is their distance.

Clearly, since these formulae follow from empirical data, it is not possible to give exact numbers for each and every case.

The Alsthom–KE design relies on forced-flow convection. Calculating h, as outlined above, gives Re = 5900 and h becomes 170 W/m^2K. The wetted perimeter is taken to be the outer surface of the conductors plus the inner surface of the tube they are in. KE comes to a far larger Re and consequently to a higher value for h: 960 W/m^2K. Instead of the surface of the conductors they calculate a virtual wetted perimeter, represented by a number of cylindrical tubes. However, even using their assumptions on the Re calculation, the design as presented by KE is **not** cryogenically stable. Their comment is that a prototype is needed, and the He flow can be increased, if necessary.

The OI design relies on natural convection. They calculate the heat exchange for the case of a single wire in a tube. The outcome is an h of 217, which was confirmed. The big question is whether the single wire calculation is applicable to a whole bundle of cables, even though relatively open. This can only be shown by a prototype.

MIITS – Adiabatic temperature rise

This term is also used in the White book and stems from a number of publications concerning superconducting wires. It stands for the integral one calculates when estimating the adiabatic temperature rise. The Joule energy deposition at every instance of the discharge is given by $P = I^2R$, and is equal to the enthalpy change of the wire $\Delta H = C(T)\Delta T$. Or, slightly different:

$$\int_{t_0}^{\infty} I^2 \, dt = A^2 \rho_m \int_{T(t_0)}^{T\infty} \frac{c(T)}{\rho(T)} dT \quad .$$

The SI units of the left integral are $[A^2s]$, those of the right expression are $[J/\Omega]$. The MIITS units can be explained as follows: 1 [MIITS] = 1$[MA^2s]$ = 10^6 $[A^2s]$. For the right-hand integral, tables were presented in [4], in $[MIITS/cm^4]$ for different Cu qualities, for different temperature increases. Knowing these and the discharge pattern given by the left-hand integral, it becomes easy to calculate the necessary cross-section to limit the temperature in case of a discharge.

Supercritical He

See Fig. A.2: P-T diagram of He. When the temperature of He is higher than the critical temperature, there will be no condensation, the He will be vapour, single-phase only.

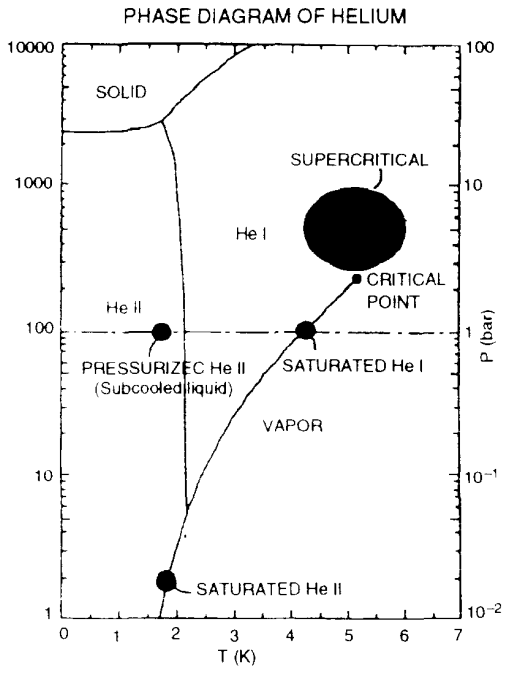

Fig. A.2

Superfluid He

See Fig. A.2. When cooling He^4 below 2.15 K, a phase change occurs. This is the so-called lambda point. The heat capacity and conductivity rise to very large values. Physically this transition corresponds to Bose condensation. This means that all atoms go

into the same quantum state corresponding to the lowest energy. This state is very comparable to superconductivity. Heat is conducted as a wave, and heat diffusion no longer applies. The He moves seemingly frictionless up to a certain speed. Superfluid He will be used for cooling the LHC magnets.

Superinsulation

Insulation material to reduce heat influx by radiation. Consists of a number of metallic layers, normally Al foils, interspaced by a polymer. Care must be taken to avoid thermal shorts which reduce the effectiveness of the superinsulation.

Kapton®

Trademark of Dupont for polyimide products. Good radiation-resistant properties, applicable for low temperatures.

Mylar®, Kevlar®

Tradenames for polymer fibre materials, characterized by their strength.

Stilan

Tradename for polyarylene. Extrudable polymer with favourable properties at low temperatures. Radiation tests are being performed.

HEPAK

See following introduction message:

Thermodynamic, transport, superfluid, and lambda line properties of helium for temperatures from 0.8 to 1500 K with pressures to 20000 bars including liquid-vapor mixtures.

Version 3.21 Numerical output is consistent with helium properties in NIST Technical Note 1334 (revised and scheduled to be reprinted by NIST in 1992). Viscosity, surface tension, refractive index, and near-critical saturation properties from NIST TN 1334 (1989) and earlier versions of HEPAK have been revised jointly by NIST and CRYODATA.

Program written by V. ARP, R.D. MCCARTY, and B.A. HANDS.

(C) Copyright by CRYODATA, P.O. Box 558, Niwot, CO 80544 . All rights reserved.

Crosstalk Considerations

The conductor layout in the KE–A proposal is sketched in Fig. A.3a. Owing to the diametrical assignment of conductors to circuits, indicated in Fig. A.3b, the mutual coupling to circuits with neighbouring conductors is maximized. Calculation of the coupled flux in the circuit with conductors AA′ induced by a current in circuit BB′ is necessary to estimate the induced voltage.

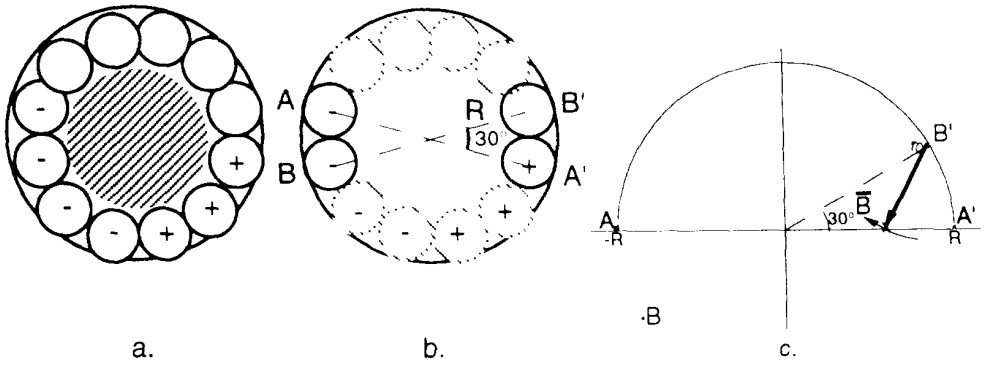

Fig. A.3: Conductor configuration.

Firstly the system of reference is changed, to have AA′ on the x-axis, as in Fig. A.3c. The currents are modelled as line currents, reduced to dots. The positive current direction is perpendicular into the paper. Further, equal spacing and equal angles between the conductors are assumed. Due to symmetry, the coupled fluxes of B and B′ being equal, only the flux induced by the current in B′ needs to be calculated and doubled to obtain the total.

The magnetic field, H, and thus the flux density $\overline{B}$ can be found using Maxwell's first equation. The coupled flux is given by $\Phi = \iint_A \overline{B} \cdot \overline{n} dA$, in general. Only the normal component of B to the surface is important, which is now B_y, a result of the choice of our reference system. B_y between A and A′ can be expressed by

$$B_y(x,0) = \frac{\mu i (x - x_{B'})}{2\pi\left[y_{B'}^2 + (x - x_{B'})^2\right]} .$$

The coordinates of B′ are (R cos 30, R sin 30). The flux per metre from A to A′ is now given by

$$\frac{\Phi}{1} = 2\frac{\mu i}{2\pi}\int_{-R}^{R} \frac{x - R\sqrt{3}/2}{(R/2)^2 + (x - R\sqrt{3}/2)^2}\,dx = \frac{\mu i}{2\pi}\left\{\ln\left[\left(\frac{R}{2}\right)^2 + \left(x - R\frac{\sqrt{3}}{2}\right)^2\right]\right\}\Bigg|_{-R}^{R} = \frac{\mu i}{2\pi} \times 2.63 .$$

Although the exact method to ramp the machine is yet unknown, an estimate can be made of the maximum ramp rate. The machine will be ramped up in 20 minutes. The outer triplet quadrupoles, with 12.5 kA supply, will have a ramp rate of about 10 A/s. The induced cross-talk voltage is equal to the time derivative of the coupled flux (Maxwell's second equation). With the formula deduced above, for a length of 300 m, it becomes

$$V_{ind} = -\frac{d\Phi}{dt} = -1.58 \times 10^{-4}\,\frac{di}{dt} .$$

Since $di/dt \leq 10$ A/s, $|V_{ind}| \leq 1.58$ mV.

This can easily be reduced. With a different conductor assignment, as shown in Fig. A.4a and b, the coupled flux is the sum of the contributions by current in B and B′. In contrast with the previous geometry, these contributions now subtract from each other.

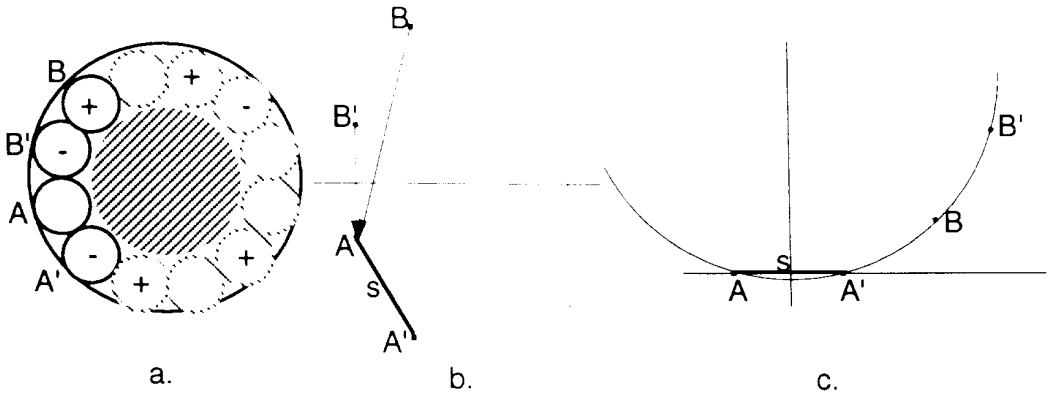

Fig. A.4: Reduction of cross-talk by different conductor assignment.

Choosing the reference such that the plane AA′ lies on the x-axis, as in Fig. A.4c, results in the following coordinates for B and B′

$$B = \left(\frac{1+\sqrt{3}}{2} S, \frac{1}{2} S \right), \qquad B' = \left(\frac{2+\sqrt{3}}{2} S, \frac{1+\sqrt{3}}{2} S \right).$$

Conveniently similar equations as before result:

$$\Phi_{B/1} = \frac{\mu i}{2\pi} \int_{-s/2}^{s/2} \frac{x - x_B}{y_B^2 + (x - x_B)^2} dx = \frac{\mu i}{4\pi} \left\{ \ln \left[y_B^2 + (x - x_B)^2 \right] \right\|_{-s/2}^{s/2}$$

$$= \frac{\mu i}{4\pi} - 1.32 \text{ (B)} \Big\| = \frac{\mu i}{4\pi} - 0.693 \text{ (B')} \quad .$$

Substitution of the respective coordinates and the notion that $i_B = -i_{B'}$, gives:

$$\Phi_{coupled} = \Phi_B + \Phi_{B'} = \frac{\mu i}{4\pi} 0.624 \times 300 = 1.87 \times 10^{-5} i .$$

This means 8.4 times less cross-talk. If necessary more can be gained, by deforming conductors. This may not be necessary, as:
– the sources are current controlled, so the control system will correct for this error and,
– compared to a ramp voltage of the order of 10 V, the error is of the order of 10^{-5}.

Cryogenic cooling

Cryogenic cooling installations absorb heat at a low temperature and reject it at a higher temperature. Cooling of He gas normally involves one or more compression and expansion stages. One of the elementary processes to do so is the Brayton cycle (Fig. A.5). It consists of adiabatic compression and heat extraction, isobaric cooling, adiabatic expansion and heat absorption, isobaric heating. A counter flow heat exchanger pre-cools the high pressure gas before expansion and pre-heats the low pressure gas before compression. The Brayton cycle is suitable for large power plants (> 500 W at 100 K), because the efficiency of the compression and expansion processes is difficult to maintain when scaling down.

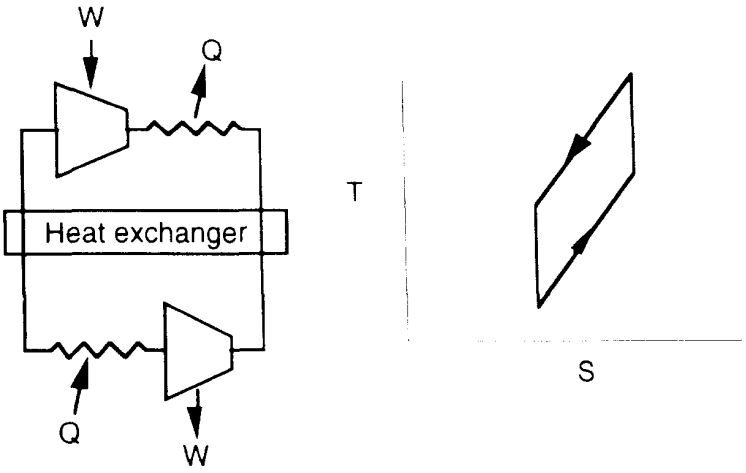

Fig. A.5: Brayton cycle.

If liquid He is required, the Joule-Thomson expansion is commonly used (see Fig. A.6). The processes are: isothermal compression, isobaric cooling, isenthalpic expansion, causing the existence of liquid, isobaric heating. The Joule–Thomson expansion is an isenthalpic process, it is irreversible and therefore generates entropy.

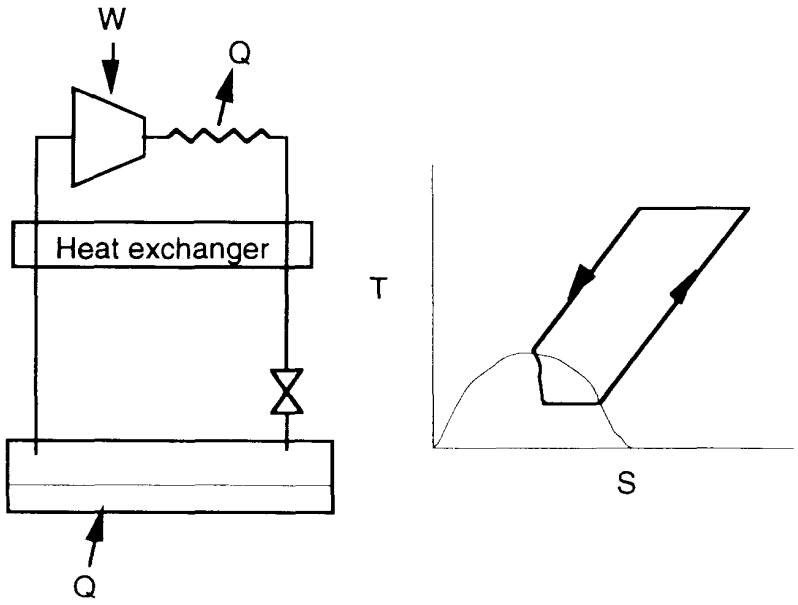

Fig. A.6: Joule–Thomson expansion for liquefaction.

These two processes can be combined, giving the Claude process (Fig. A.7). This is, in principle, the process used by the LEP cryoplants, which will also be used for the LHC.

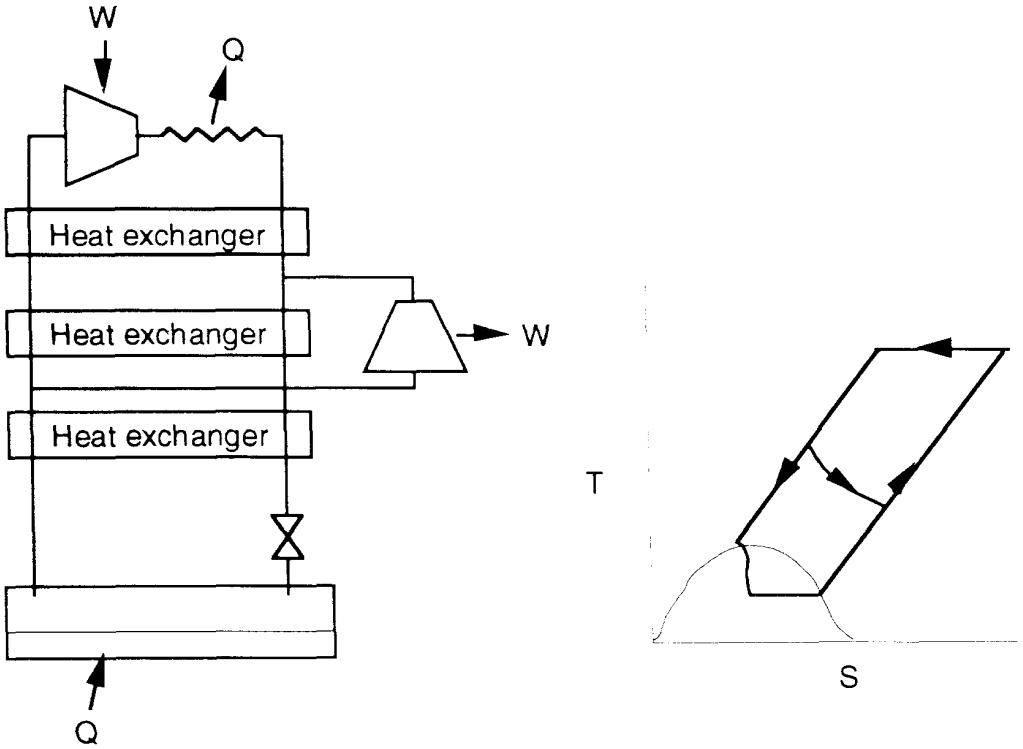

Fig. A.7: Claude cycle of liquefaction.

APPENDIX B

Verification of formulae used by KE–Alsthom

Some words of caution concerning the KE–Alsthom calculations: some of the symbols used have non-standard meanings, for example G for the dissipated heat, and Q for heat flow per surface area.

In their report §3.1 a Cu/SC ratio, Rs, is derived, as well as the conductor diameter, D. They mention it being based on setting G = Q, but the formula presented is based on $Q\pi D = G$:

$$J_{Cu} = J_c \frac{1}{Rs},$$

$$G = \rho_{cu} J^2 \frac{\pi D^2}{4} \frac{Rs}{Rs+1} = \rho_{cu} J_c^2 \frac{\pi D^2}{4} \frac{1}{Rs(Rs+1)} .$$

Rs:

$$Q\pi D = G \Rightarrow Q^2 = \rho_{Cu}^2 J_c^4 \frac{D^2}{4^2} \left[\frac{1}{Rs(Rs+1)}\right]^2 \Leftrightarrow$$

$$Q^2 = \rho_{Cu}^2 J_c^3 \frac{1}{4\pi} \left[\frac{1}{Rs^2(Rs+1)}\right] I_c \Leftrightarrow Rs^2(Rs+1) = \frac{\rho_{Cu}^2 J_c^3}{4\pi Q^2} I_c .$$

D:

$$Q\pi D = \rho_{Cu} J_c^2 \frac{\pi D^2}{4} \frac{1}{Rs(Rs+1)} \Rightarrow D = \frac{4Q}{\rho_{Cu} J_c^2} Rs(Rs+1) .$$

Adiabatic temperature rise

In the report two final temperatures are mentioned, 300 and 450 K, giving different Rs and conductor sizes. The values mentioned for Rs are 59 and 53.5. A check using MIITS tables gives 61.2 and 57, respectively.

Calculation for the pitch of the helix

The length over one pitch of a conductor wound in a helical shape, with a constant radius, R, can easily be determined. When changing the coordinate system from cartesian to cylindrical coordinates, the helix becomes a straight line in the plane r = R. The length can then be determined by:

$$L^2 = P^2 + 4\pi^2 R^2,$$

P: pitch height,
L: length,
R: radius.

This can be transcribed to represent the pitch. The pitch is supposed to be constant when the length of the wire and the radius change during cooldown.

Derivation of the pitch of one lead wound around the shrinking element, under the condition of no change of pitch during contraction of the wire goes as follows:

$$P^2 = L_w^2 - (\pi d_w)^2 = L_c^2 - (\pi d_c)^2 = (1-y)^2 L_w^2 - (\pi d_c)^2$$

$$\Rightarrow [(1-y)^2 - 1]L_w^2 = (\pi d_c)^2 - (\pi d_w)^2 \Leftrightarrow L_w^2 = \frac{(\pi d_c)^2 - (\pi d_w)^2}{[(1-y)^2 - 1]}.$$

$$P^2 = \frac{(\pi d_c)^2 - (\pi d_w)^2}{[(1-y)^2 - 1]} - (\pi d_w)^2 = \frac{(\pi d_c)^2 - (\pi d_w)^2}{[(1-y)^2 - 1]} - \frac{[(1-y)^2 - 1](\pi d_w)^2}{[(1-y)^2 - 1]}$$

$$= \frac{(\pi d_c)^2 - (1-y)^2(\pi d_w)^2}{[(1-y)^2 - 1]} \Rightarrow P = \pi d_w \sqrt{\frac{\left(\frac{d_c}{d_w}\right)^2 - (1-y)^2}{(1-y)^2 - 1}}.$$

P: pitch,
d_W: warm diameter of the shrinking element,
d_C: cold diameter of the shrinking element,
L_W: warm length of the lead,
L_C: cold length of the lead,
y: relative shrinkage of the lead (normally referred to as 1),
μ: winding angle with respect to central axis.

The formula given for μ in the report could not be confirmed. Another expression can be derived, using Fig. B.1 as an aid:

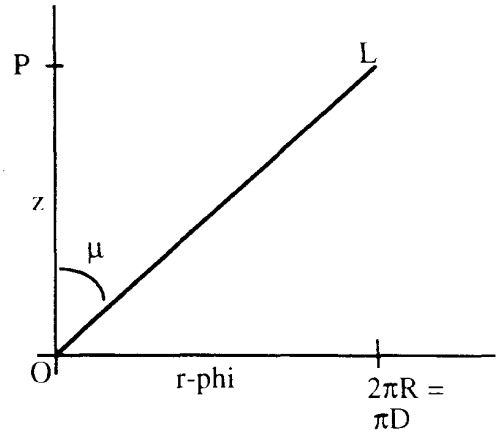

$$\sin\mu = \frac{\pi d_w}{L_w}$$

$$\text{or } \operatorname{atn}\mu = \frac{\pi d_w}{P}$$

Fig. B.1: Winding angle.

It can be seen that the winding angle changes when the conductor and core contract. This is an error in the report, although not serious. The warm and cold angles, with the pitch and core diameter as stated of 150 mm and 20 mm, are 22.7° and 22.1°. The report states 24°.

The report mentions the radial movement and distance between wires. The formula used was not confirmed, but with a slightly different approach the same numbers are obtained. It is not clear why in the formula presented the distance change between the wires depends on Rc, the cold wire radius. The following drawing (Fig. B.2) shows the geometry and change due to contraction of the shrinking element.

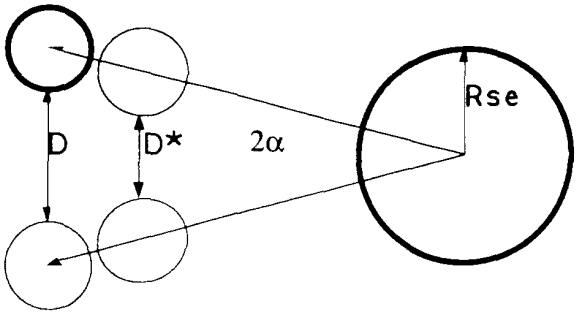

Fig. B.2: Distance variation during cool-down.

The difference between the distances is given by: $D-D^{*}= 2R_{se}K_{se} \sin \alpha$. K_{se} is the shrinking factor of the core, in other words $R_{se}K_{se}$ is the radial movement. Since the number of cables in the outer layer is 12, α is 15°. If the core shrinks radially by 0.2 mm, the report mentions a diameter change of 0.4 mm and, incorrectly, a wire movement of 0.4 mm, which should be 0.2 mm. This means a change of distance of 0.1 mm. The report mentions 0.09 mm.